

*Library copy  
R.A. 388*

Copy No. *18*  
RM No. SL8G02

1948

CLASSIFIED

UNCLASSIFIED

# NACA

*H.L. Dryden* Date *6-11-53*  
*per NACA Release form #1477. By HLR, 7-16-53*  
**RESEARCH MEMORANDUM**

for the

Bureau of Aeronautics, Department of the Navy

TANK TESTS OF A POWERED MODEL OF A COMPRESSION PLANE -

NACA MODEL 171A-2

By

Elmo J. Mottard and Robert D. Ruggles

Langley Aeronautical Laboratory  
Langley Field, Va.

CLASSIFIED DOCUMENT

This document contains classified information affecting the National Defense of the United States within the meaning of the Espionage Act, USC 50:31 and 32. Its transmission or the revelation of its contents in any manner to an unauthorized person is prohibited by law. Information so classified may be imparted only to persons in the military and naval services of the United States, appropriate civilian officers and employees of the Federal Government who have a legitimate interest therein, and to United States citizens of known loyalty and discretion who of necessity must be informed thereof.

## NATIONAL ADVISORY COMMITTEE FOR AERONAUTICS

WASHINGTON

JUL 8 1948



NATIONAL ADVISORY COMMITTEE FOR AERONAUTICS

RESEARCH MEMORANDUM

for the

Bureau of Aeronautics, Department of the Navy

TANK TESTS OF A POWERED MODEL OF A COMPRESSION PLANE -

NACA MODEL 171A-2

By Elmo J. Mottard and Robert D. Ruggles

SUMMARY

The compression plane is intended for operation on or close to the surface of the water, and has a hull with a concave bottom which forms the upper surface of a tunnel into which air is forced under pressure to support part of the load.

The results of the tests made in Langley tank no. 1 include values of the horizontal forces, trimming moment, and static pressure in the tunnel for a wide range of loads and speeds and two power conditions, and are presented in the form of curves against speed with load as a parameter. The results are scaled up to 10 times the model size for three conditions at which the model is self-propelled at a steady speed.

Lift is obtained from the static pressure of air in the tunnel. In general, the ratio of the gross load to the total resistance increases with increase in load and decrease in speed. This ratio varies between 1.7 and 5.7 at high speeds and has a maximum value of 7. The total resistance is nearly the same for both power conditions except at low speeds and heavy loads. No abrupt change in forces on the hull or flow around the hull occurs in the region of zero draft.

The centers of pressure are generally far aft. At the most efficient trim ( $1.2^\circ$ ), considerable bow-up moment would be required for practicable operation.

There is no abrupt transition from the air-borne to the water-borne condition.

## INTRODUCTION

The compression plane is intended for operation on or close to the surface of the water and has a hull with a concave bottom which forms the upper surface of a tunnel into which air is forced under pressure to support part of the load. Previous tests of a compression plane (NACA model 171) are described in reference 1.

The Bureau of Aeronautics requested additional tests of the compression plane, with certain modifications desired by its inventor, Mr. D. K. Warner, to further evaluate the principle of operation of the compression plane and to supply additional information on its operation at very shallow draft and high speed, that is, operation while skimming on the surface of the water. Consequently, model 171 was modified and tested in Langley tank no. 1 as model 171A-2.

## DESCRIPTION OF MODEL

Model 171A-2 is shown in figures 1 and 2. The photograph of the model mounted on the towing gear (fig. 2(a)) was taken before the fairings were installed around the air scoops and towing fitting; figures 2(b), 2(c), and 2(d) show the model with these fairings.

Model 171A-2 is the result of the following modifications to model 171:

1. Plywood sides were added, which appreciably increased the height of the model and the depth of the tunnel, and slightly increased the beam and length.
2. A plywood bottom, or closure, was installed which completely closed the bottom of the tunnel for a distance of about twenty inches behind the propellers. This forward closure, which directed the propeller slipstream into the tunnel, fitted closely around the propellers so as to prevent loss of pressure. Under some conditions the bottom of the closure served as a forward planing surface.
3. A planing plate was added at the rear. This plate was set at a greater angle with the water surface than the bottom of the original model. It had an airfoil-shaped upper surface which formed the bottom of a slot through which air escaped from the tunnel.
4. Variable-frequency induction motors were substituted for the DC-series motors formerly used, and propellers with wide blades and a high pitch were installed to increase the thrust.

5. The towing pivot was moved forward and up to provide space for a moment dynamometer.

6. In order to improve the air flow over the top of the model, the safety mast was moved from its location forward to a position aft of the towing pivot, and the scoops to supply cooling air for the motors were moved from the top to the sides.

### APPARATUS AND PROCEDURE

Langley tank no. 1 and the towing carriage are described in reference 2. The model suspension and the apparatus for measuring forces and moments are shown diagrammatically in figure 3.

The model was tested at two power conditions corresponding to static thrusts of 7.3 and 12 pounds. The higher power was obtained with three-blade, 9-inch-diameter (cut down from 10-inch-diameter), 14-inch-pitch wooden propellers rotating at approximately 10,700 rpm. The lower power was obtained with three-blade, 9-inch-diameter (cut down from 10-inch-diameter), 10-inch-pitch wooden propellers rotating at approximately 11,600 rpm. The lower power condition is the same as that used in the tests described in reference 1. Throughout the tests the rotational speed of the propellers was held within limits which resulted in a variation in static thrust (thrust with zero forward speed) of less than  $\pm 0.1$  pound. Power-input measurements were made on the two motors simultaneously over the range of speeds and loads covered by the tests.

Special tests were made to determine the true propeller thrust (propeller-shaft tension) as a function of airspeed for negative draft conditions. In these tests the thrust was obtained by measuring the horizontal force on the entire motor assembly, which was enclosed within an independently supported streamline fairing and mounted on the towing carriage.

As the result of preliminary tests to determine the trim for minimum resistance (fig. 4), an angle between the base line and the water of  $1.2^\circ$  was selected for the remainder of the tests. It will be noted that the power condition for figure 4 corresponds to 13 pounds static thrust instead of the usual 12 pounds for the high-power condition; the data presented in this figure were obtained before a method was devised for accurately controlling the rotational speed of the propellers. The position of the rear planing plate shown in figure 1 was chosen by Mr. Warner on the basis of preliminary tests (table I), made under his direction, in which the plate was rotated about its trailing edge.

Tests of the model in the water were made by the general (constant load) method; tests in the air and at shallow drafts were made with

constant draft. Values of lift (load), draft, trimming moment, towing force, and static pressures were obtained for a range of speeds and loads and both power conditions. The draft was measured to the trailing edge of the rear planing plate. The trimming moment was measured about the towing pivot. (See fig. 1.) The towing force is the resultant horizontal force of the model as measured on the resistance dynamometer. The towing gear was shielded to minimize windage, and windage tares were deducted from all horizontal force measurements. Static pressures relative to the free air were measured at points along the center line of the tunnel by means of static-pressure tubes located in the tunnel. (See fig. 1.)

## RESULTS AND DISCUSSION

### Tests at Constant Load

Towing force and draft.- With the high-power condition, an accelerating force (negative towing force) is acting at all loads over most of the speed range. (See fig. 5(a).) With a load of 75 pounds this accelerating force becomes zero at 65 feet per second. With the low-power condition (fig. 5(b)), the accelerating force is zero at a much lower speed. The draft is greater with the low power than with the high power. The towing force and draft curves of figures 5(a) and 5(b) do not show any very abrupt changes in the region of zero draft; and if discontinuities occur in this region, they are hidden by the scatter of the data.

Static pressure in tunnel.- The static pressures (fig. 6) are generally positive except for the most forward orifice (orifice no. 1, just forward of the trailing edge of the forward closure). Where negative pressures occur, they decrease in magnitude with increase in load and increase in magnitude with increase in speed.

Trimming moment.- The trimming moments are shown in figures 7(a) and 7(b). Moments which tend to raise the bow are considered positive. At high speeds the moments are negative and of considerable magnitude, indicating that the centers of pressure are well aft on the hull. At 70 feet per second and 75 pounds load with the high-power condition (fig. 7(a)) the trimming moment is -72 pound-feet; the corresponding center of pressure is approximately 70 percent of the model length aft of the bow. Figure 4 indicates that the moment becomes more positive as the trim is decreased; but even at zero trim, where the load must be limited to 40 pounds to prevent water from entering the propeller disks, the center of pressure is behind the center of moments (the center of moments is 59 percent of the model length aft of the bow).

Observations of flow and stability.- At light loads and high speeds, where the model does not make contact with the water, the roughness of the water surface produced by the propeller slipstream largely obscures the wake. Without power the wake is clearly discernible, even at negative drafts of 2 or 3 inches.

Over most of the speed and load range, air is forced out from under the model, carrying spray with it, so that the tunnel is not completely sealed by contact with the water surface. The transition from positive to negative draft is gradual: no abrupt change in the behavior of the model in the range of zero draft is apparent, and vertical instability of the type frequently encountered with planing plates at fixed trim and shallow draft (reference 3) does not occur with power, although it does occur without power.

The forward closure contacts the water only at the highest load and very low speeds; under these conditions vertical instability with fixed trim is encountered, which appears to be associated with the alternate opening and closing of the gap between the rear edge of the front closure and the water surface. The model rises until the front closure breaks the surface, allowing air to escape from the tunnel, then falls, and the cycle is repeated.

#### Tests at Constant Draft

The towing force and total lift obtained from tests at constant draft with the high power for speeds of 30, 50, and 70 feet per second are plotted against draft in figure 8. The curves are extended from zero draft to 1-inch draft, using data obtained from tests at constant load, to show clearly the relationship at zero draft. Because of lack of sufficient lift measurements at specific speeds of 30, 50, and 70 feet per second, the curves of lift against draft are obtained from cross plots of lift and draft against speed.

Neither figure 8 nor figures 5(a) and 5(b) show any abrupt change in either lift or towing force in the region of zero draft. The smooth transition from water to air is attributed to the fact that the water surface is not well defined because of the roughness caused by air escaping from beneath the model.

#### Power

There is no apparent variation of power input to the propeller motors with load or draft. (See fig. 9.) Even closing the tunnel bottom and slot so as to completely seal the tunnel except for the opening behind the propellers has no appreciable effect on the power input.

The power-input curves give a misleading impression of the power required for the compression plane because the efficiencies of the motors and propellers are much lower than the efficiencies usually associated with electric motors and aircraft propellers.

The curves of propeller-shaft tension against speed (fig. 10) for the two power conditions afford a means of determining the operational thrust coefficients and thence, from the data of reference 4, of estimating propeller efficiencies and power requirements for an optimum installation. The maximum efficiencies indicated from reference 4, and the corresponding power input to the propellers, determined as

$$\frac{\text{Thrust horsepower}}{\text{Propeller efficiency}} = \frac{VT}{550 \times \text{propeller efficiency}}$$

where

T thrust (propeller-shaft tension), pounds

V forward velocity, feet per second

are presented in table II for model data at three test conditions of zero towing force. The three conditions are marked A, B, and C in figures 5(a) and 5(b).

As evidence that these propeller efficiencies are approximately as high as can be reasonably expected for these thrust coefficients, the ideal efficiencies are also included in the table for comparison. The ideal efficiency is obtained from the following relations (reference 5, pp. 203 and 204):

$$\text{Ideal efficiency} = \frac{1}{1 + a}$$

where

$$1 + 2a = \sqrt{1 + \frac{8C_T}{\pi}}$$

$$C_T = \frac{T}{\rho V^2 D^2}$$

T thrust (propeller-shaft tension), pounds

$\rho$  density of air, slugs per cubic foot

V forward velocity, feet per second  
D diameter of propeller, feet

### Resistance

The total resistance, which is composed of the frictional and wave-making resistance of the water and the aerodynamic resistance, including the effect of the propeller slipstream (in short, the sum of all forces opposing forward motion), is related to the thrust and towing force as follows:

$$\text{Total resistance} = \text{Towing force} + \text{thrust}$$

where the thrust is the propeller-shaft tension at the test condition. The total resistance, as a function of speed, presented in figures 11(a), 11(b), and 12, is the sum of the towing force, figures 5(a) and 5(b), and the thrust, figure 10, and is therefore based upon the assumption that the thrust presented in figure 10 is the same as that at the actual test condition.

The total resistance is plotted against speed in figures 11(a) and 11(b) together with the corresponding load-resistance ratio  $\Delta_0/R_T$ . In general, the ratio increases with increase in load and decrease in speed. If speeds below 15 feet per second are not considered, the maximum ratio of 7 occurs with a load of 60 pounds at 33 feet per second with the high-power condition.

At the highest speed tested, 70 feet per second, the ratio varies from 1.7 to 5.7, depending on the load. Figure 12, where the total resistances and drafts for the high- and low-power conditions are compared, shows that the total resistance is nearly the same for both power conditions, except at low speeds and heavy loads.

### Extrapolation to Full Size

The only known method of extrapolating the results from the model tests of the compression plane to larger sizes and higher speeds is afforded by Froude's Law of Comparison for geometrically similar bodies. An explanation of Froude's Law and its application to model testing may be found in chapter 3.1 of reference 6 and other classic literature on the principles of similitude. If Reynolds number and other effects are neglected, the physical quantities of interest in the performance of the compression plane are related to its linear dimensions (reference 6) as follows:



Length . . . . .	$L$
Linear velocity . . . . .	$L^{\frac{1}{2}}$
Force, resistance, or weight . . . . .	$L^3$
Work, energy, or torque . . . . .	$L^4$
Power . . . . .	$L^{\frac{3}{2}}$
Pressure per unit area . . . . .	$L$

It follows that by substituting  $\lambda$ , the ratio of full-size length to model length, for  $L$ , the factors for converting the data from the model tests to a geometrically similar compression plane are obtained.

By means of these conversion factors, model data for the three zero-towing-force test conditions of table II have been converted to correspond to hulls of ten times the model size, operating at maximum speed with the scale thrust. These full-scale characteristics are shown, together with model data, in table II. For example, at condition A the gross load and speed for the model (fig. 5(a)) are 75 pounds and 65 fps; the thrust, obtained from figure 10, is 12.8 pounds; the propeller efficiency, estimated from reference 4, is 57 percent; and the power input, obtained from the relation,

$$\text{Power input} = \frac{VT}{550 \times \text{propeller efficiency}}$$

is 2.65 horsepower. Assuming a model scale  $1/\lambda$  of one-tenth and applying Froude's Law, it appears that at condition A a design (geometrically similar to the model) with a length of 92 feet, a beam of 9.2 feet, and a gross load of 75,000 pounds would require 8,480 horsepower for a maximum speed of 206 fps (140 mph).

The foregoing method of scaling the data yields values for the various full-size physical quantities (length, width, power, etc.) which are definitely related to each other and to the corresponding physical quantities of the model. No rigorous method is apparent whereby the physical quantities may be scaled independently of each other or according to any relationships other than those used. For example, the performance of a compression plane having length-beam ratio different from that of the model could not be determined from these data.

## CONCLUDING REMARKS

Lift is obtained from the static pressure of air in the tunnel over a large range of loads.

Except at heavy loads and low speeds, the total resistance is nearly the same for both power conditions, and the gross-load total-resistance ratio  $\Delta_o/R_T$  increases with increase in load and decrease in speed. The gross-load total-resistance ratio varies between 1.7 and 5.7 at the highest speed, 70 feet per second, and has a maximum value of 7 at 33 feet per second with a load of 60 pounds at the high-power condition.

Centers of pressure are for the most part aft of the center of moments (the center of moments is 59 percent of the model length aft of the bow). Considerable bow-up moment would be required to balance the model at its most efficient trim. Optimum performance is obtained at a trim of  $1.2^\circ$ . At lower trims the towing force is slightly higher, indicating higher resistance, and the load capacity of the model is much less; at higher trims the towing force increases rapidly with the trim.

No abrupt change is apparent in either the data or the behavior of the model at or near zero draft, and the draft at which the model contacts the water is not definable.

Langley Aeronautical Laboratory  
National Advisory Committee for Aeronautics  
Langley Field, Va.



Elmo J. Mottard  
Aeronautical Research Scientist

Robert D. Ruggles  
Naval Architect

Approved:



John B. Parkinson  
Chief of Hydrodynamics Division

MLE

## REFERENCES

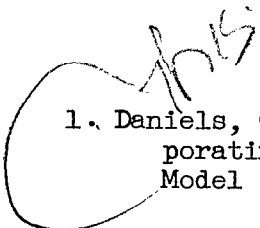
- 
1. Daniels, Charles J.: Tests of a Model of a Flying-Boat Hull Incorporating D. K. Warner's "Compression-Plane" Principle - NACA Model 171. NACA MR No. L4F24, 1944.
  2. Truscott, Starr: The Enlarged N.A.C.A. Tank and Some of Its Work. NACA TM No. 918, 1939.
  3. Shoemaker, James M.: Tank Tests of Flat and V-Bottom Planing Surfaces. NACA TN No. 509, 1934.
  4. Biermann, David, Gray, W. H., and Maynard, Julian D.: Wind-Tunnel Tests of Single- and Dual-Rotating Tractor Propellers of Large Blade Width. NACA ARR, Sept. 1942.
  5. Glauert, H.: The Elements of Aerofoil and Airscrew Theory. Cambridge Univ. Press, reprint of 1942.
  6. Taylor, D. W.: The Speed and Power of Ships. Ransdell, Inc. (Washington, D. C.), 1933.

TABLE I  
DATA SHOWING TOWING FORCE AND TRIMMING MOMENT  
FOR VARIOUS SLOT HEIGHTS AND PLATE ANGLES;  
SPEED, 70 FPS; TRIM,  $1.2^{\circ}$ ; 12.7-POUND  
STATIC THRUST - NACA MODEL 171A-2

Slot height (in.)	Plate angle (deg)	Gross load (lb)	Towing force (lb)	Trimming moment (ft-lb)
$\frac{3}{8}$	20.5	75	-0.9	-63.7
$\frac{3}{8}$	20.5	45	-2.0	-60.7
$\frac{1}{2}$	19.5	60	-1.8	-50.3
$\frac{7}{8}$	16.4	45	-2.9	-42.9
1	15.3	45	-2.7	-50.3
1	15.3	60	-.8	-66.0
$1\frac{1}{8}$	14.3	45	-2.8	-45.2
$1\frac{1}{4}$	13.2	45	-2.9	-32.4





TABLE II  
MODEL AND FULL-SIZE PERFORMANCE FEATURES - NACA MODEL 171A-2

	Conversion factors	Test condition A		Test condition B		Test condition C	
		Model	Full size	Model	Full size	Model	Full size
Length, ft	$\lambda$	9.2	92	9.2	92	9.2	92
Beam, ft	$\lambda$	0.92	9.2	0.92	9.2	0.92	9.2
Load, lb	$\lambda^3$	75	75,000	45	45,000	15	15,000
Speed, fps	$\lambda^{\frac{1}{2}}$	65	206	42	133	55	174
Thrust, lb	$\lambda^3$	12.8	12,800	8.1	8,100	7.0	7,000
Thrust horsepower	$\lambda^{\frac{3}{2}}$	1.51	4,840	0.62	2,000	0.70	2,200
Ideal propeller efficiency, percent	1	65.4	65.4	58.3	58.3	69.8	69.8
Estimated actual propeller efficiency, percent	1	57	57	51	51	61	61
Estimated horsepower input	$\lambda^{\frac{3}{2}}$	2.65	8,480	1.21	3,870	1.15	3,680
Total resistance, lb	$\lambda^3$	12.8	12,800	8.1	8,100	7.0	7,000
Draft, ft	$\lambda$	0.087	0.87	0.092	0.92	-0.002	-0.02
Trimming moment, lb-ft	$\lambda^4$	-68.7	-687,000	-53.6	-536,000	-23.6	-236,000
Pressure in tunnel, orifice no. 2, lb/sq ft	$\lambda$	7.4	74	3.4	34	-1.4	-14



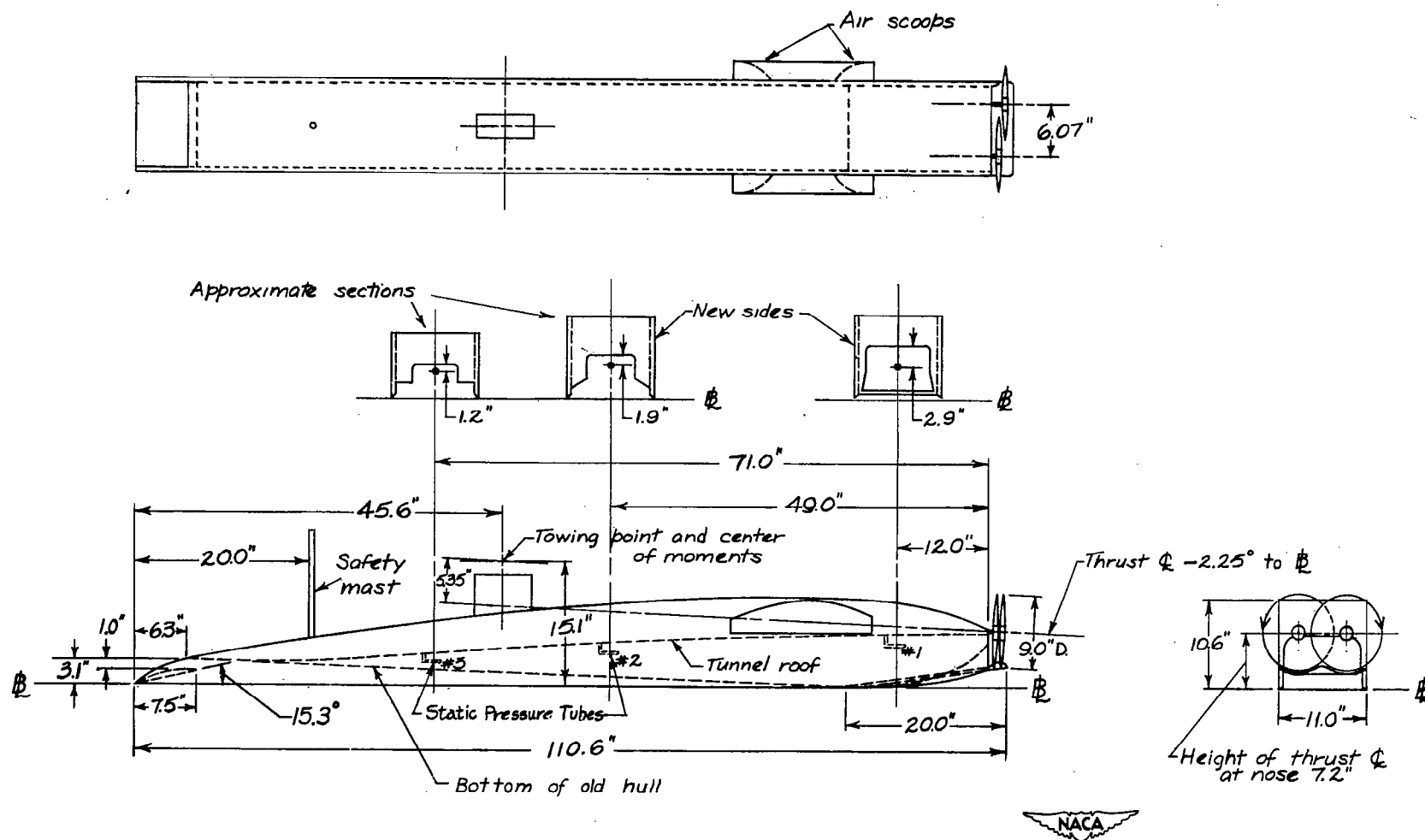
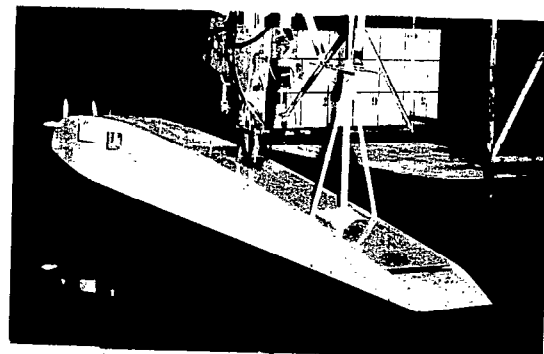
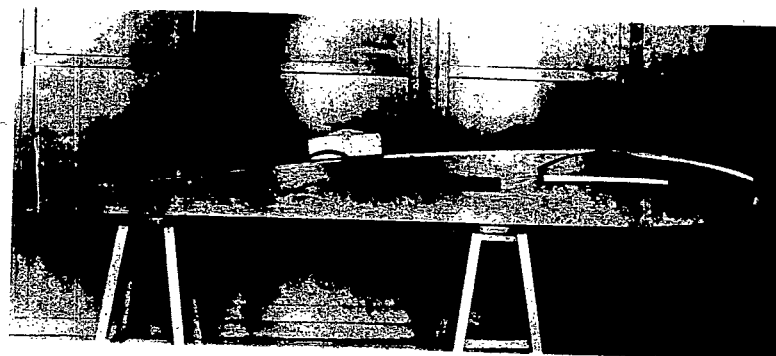


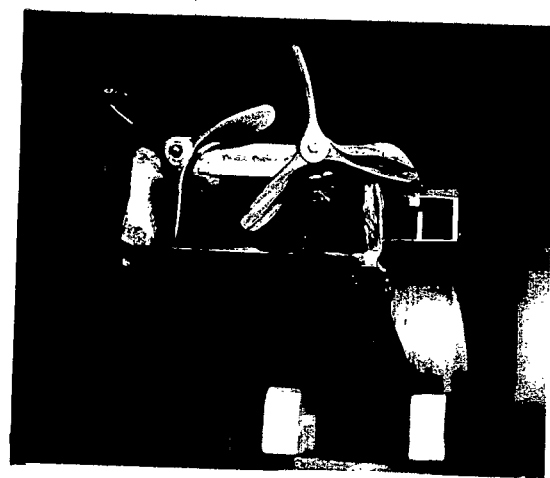
Figure 1.- Model 171A-2. General arrangement.



(a) Model on towing gear.



(b) Profile view.



(c) Front view.



(d) Three-quarter front view.

Figure 2.- Photographs of model 171A-2.



2530

NACA RM No. SL8G02

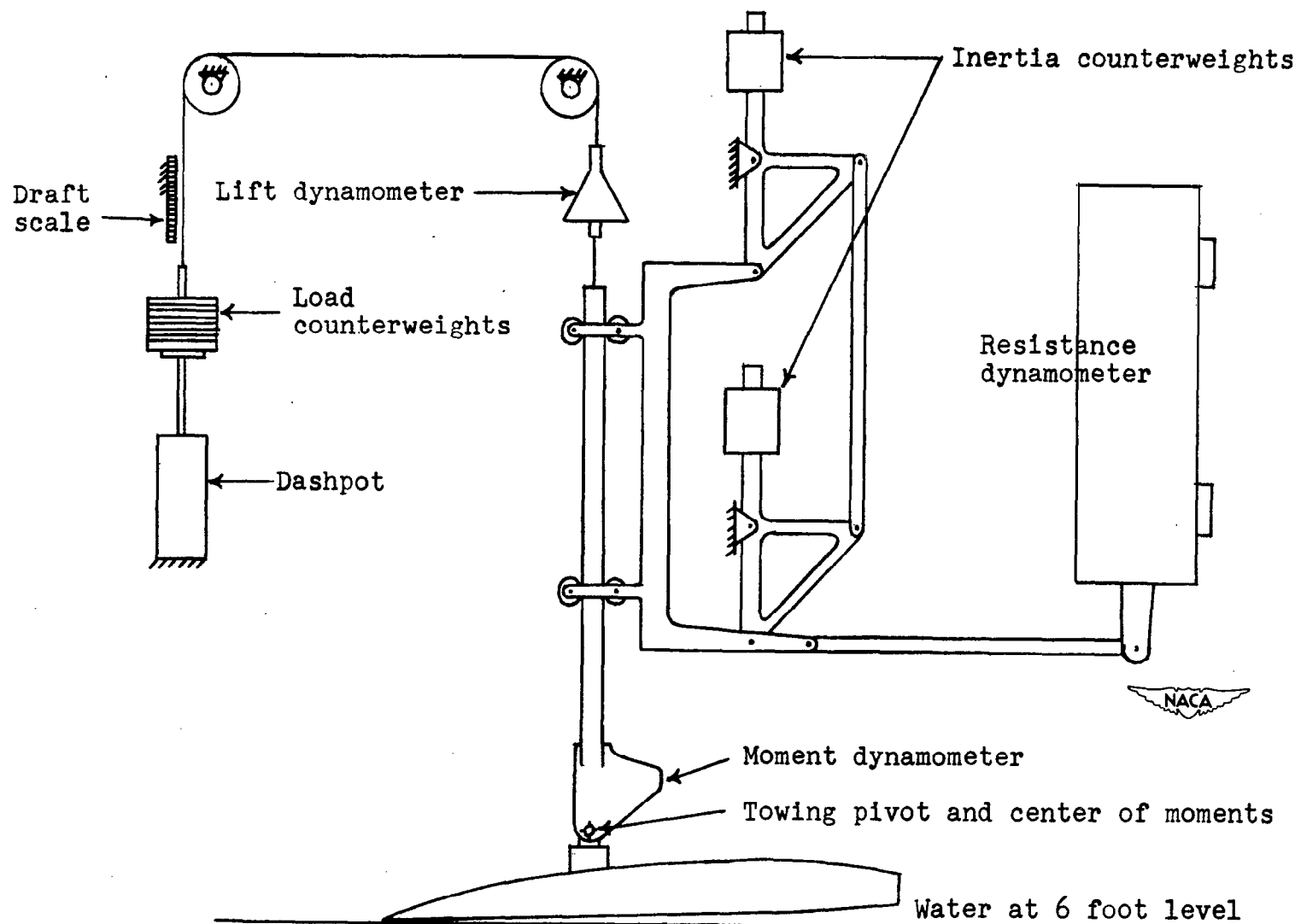


Figure 3.- Diagrammatic sketch of apparatus. Model 171A-2.



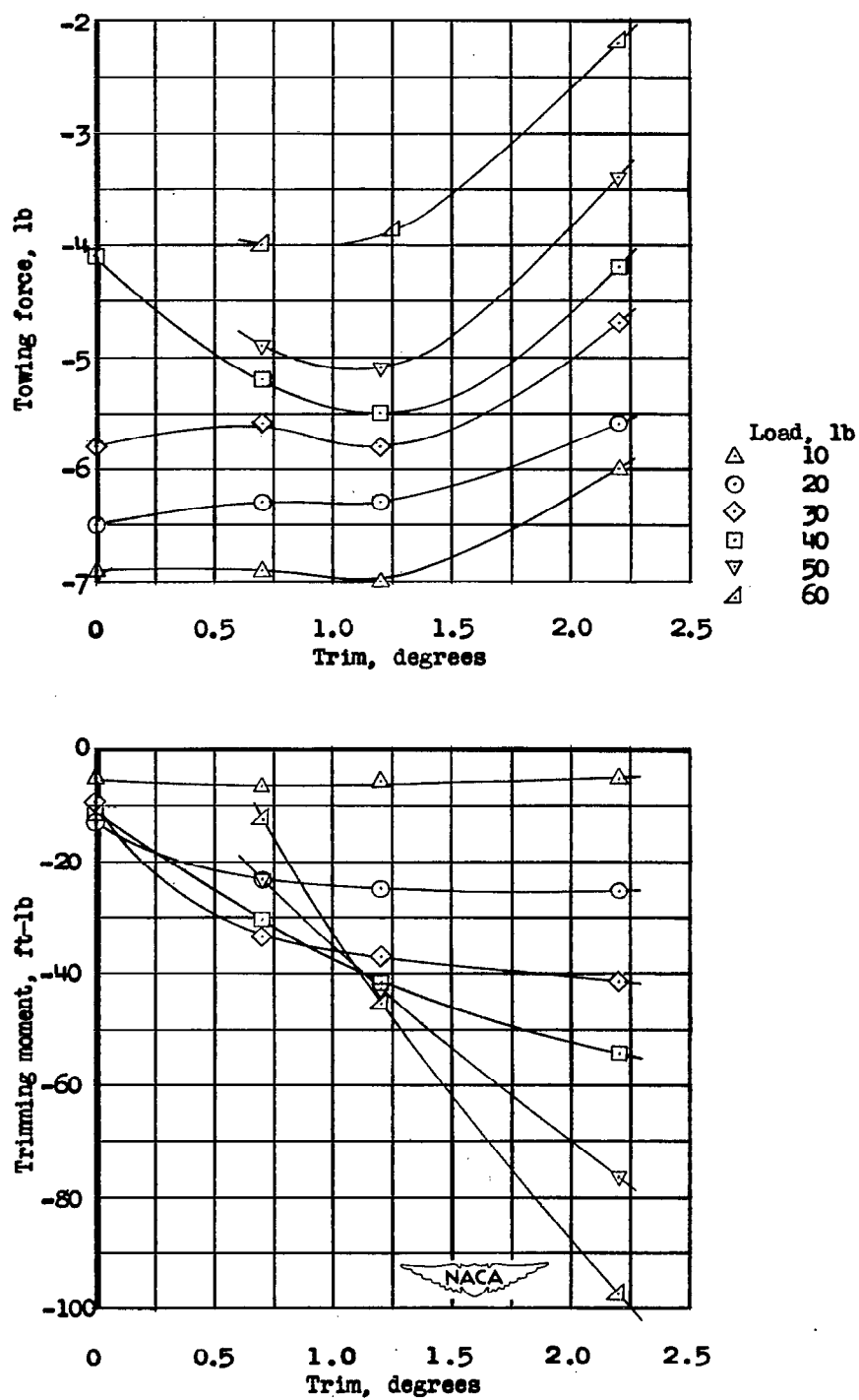
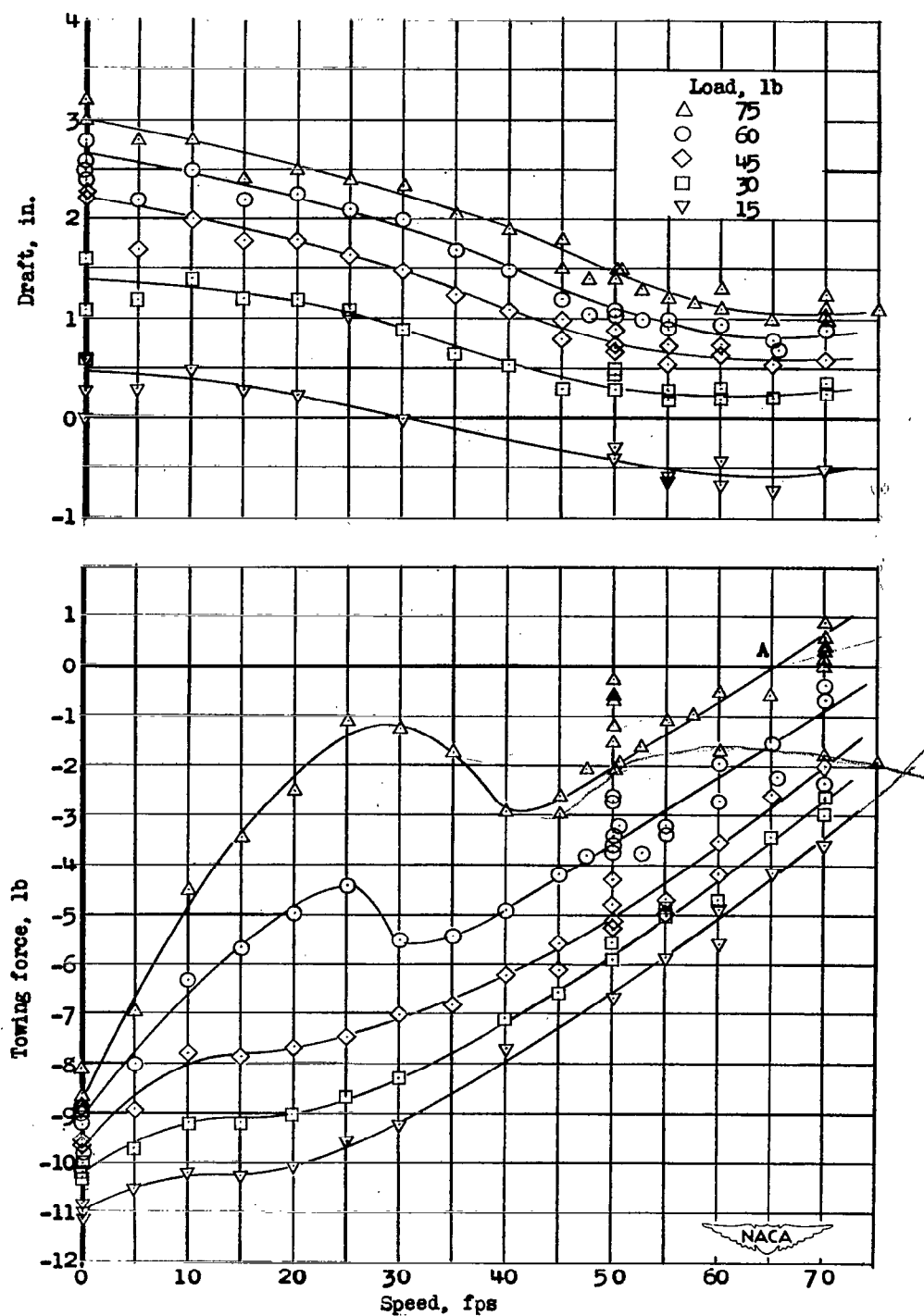
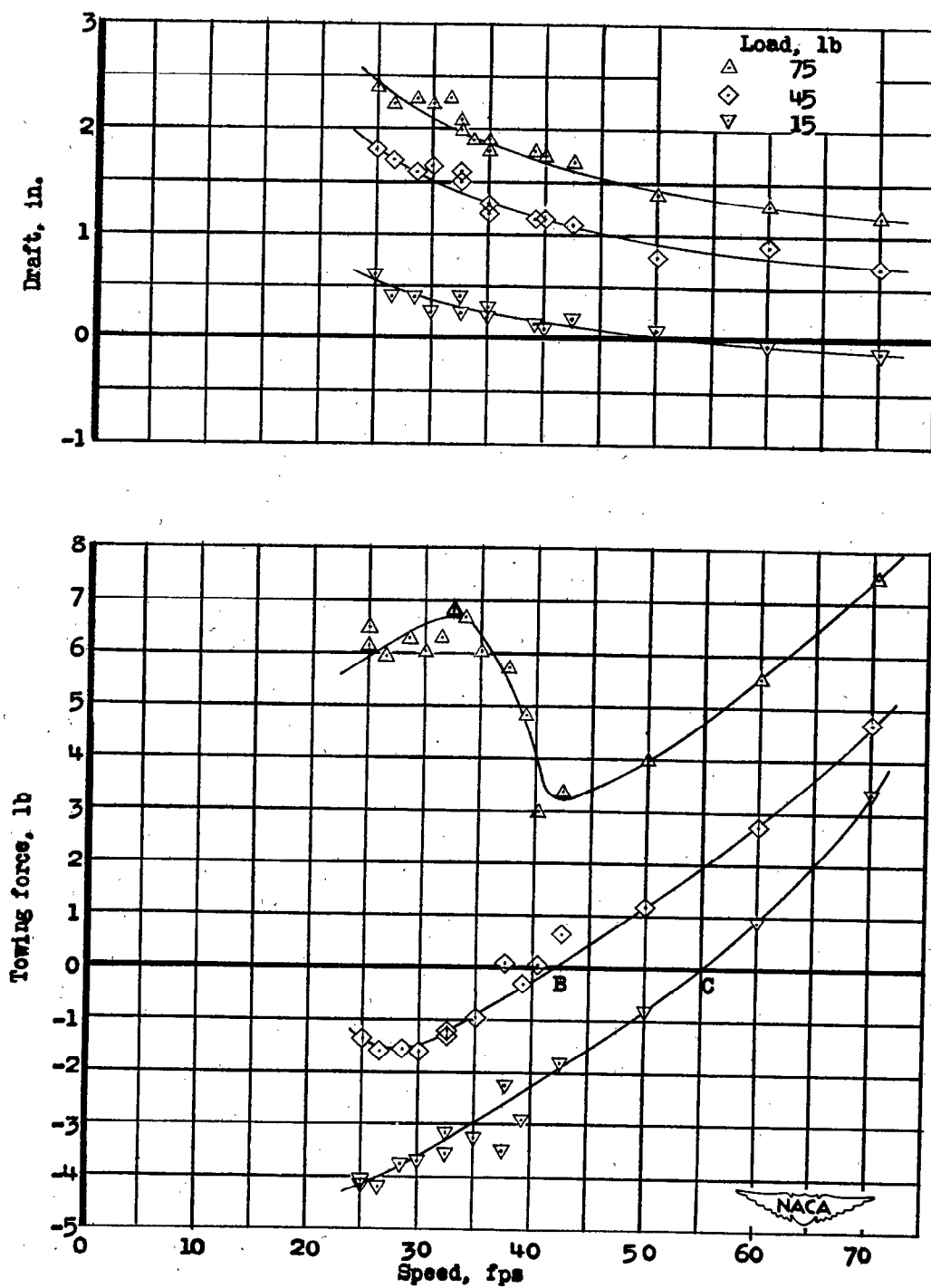


Figure 4.- Variation of towing force and trimming moment with trim; speed, 50 fps; 13-pound static thrust; slot thickness, 3/8 inch. Model 171A-2.



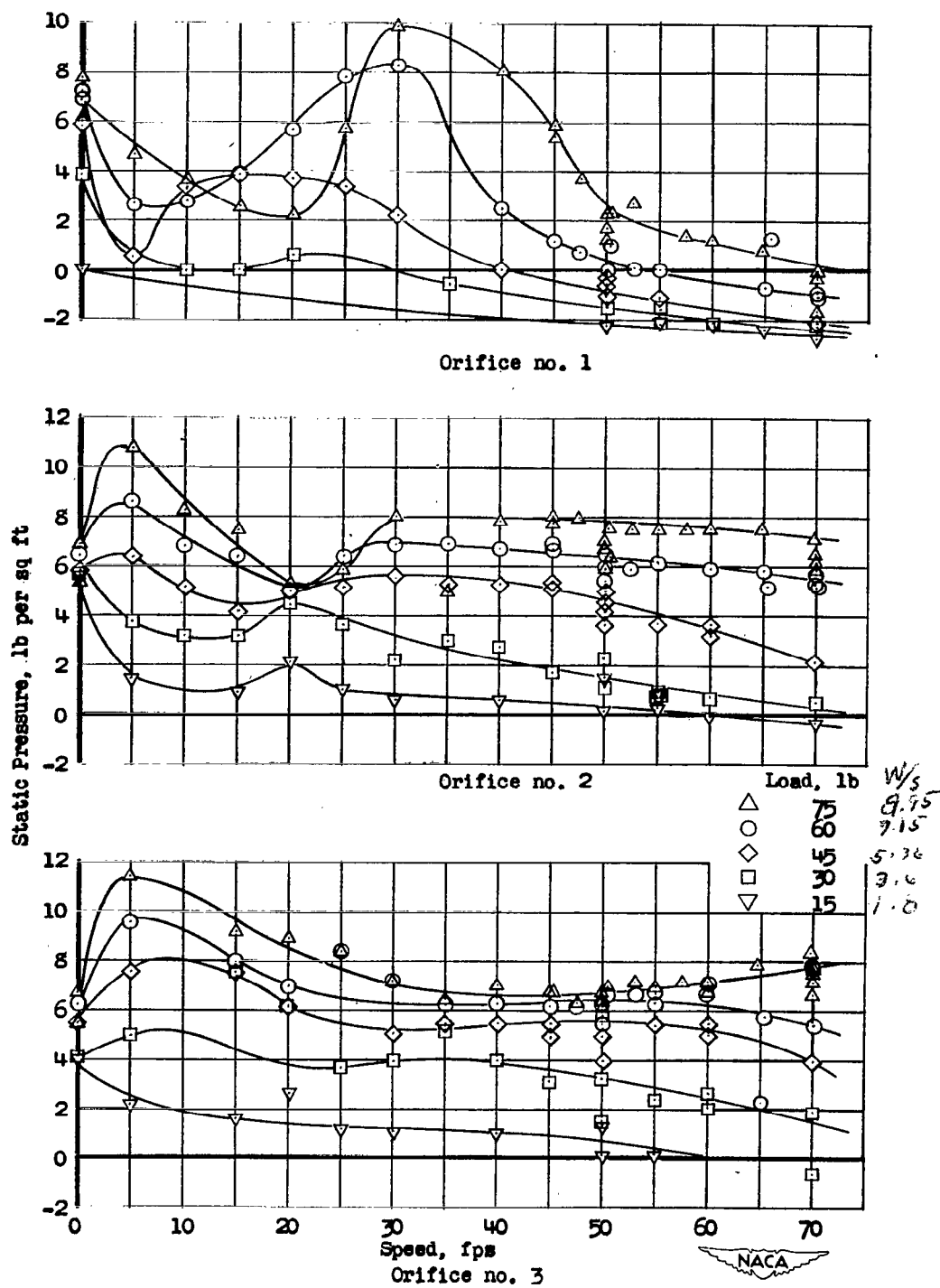
(a) High-power condition.

Figure 5.- Variation of towing force and draft with speed. Model 171A-2.



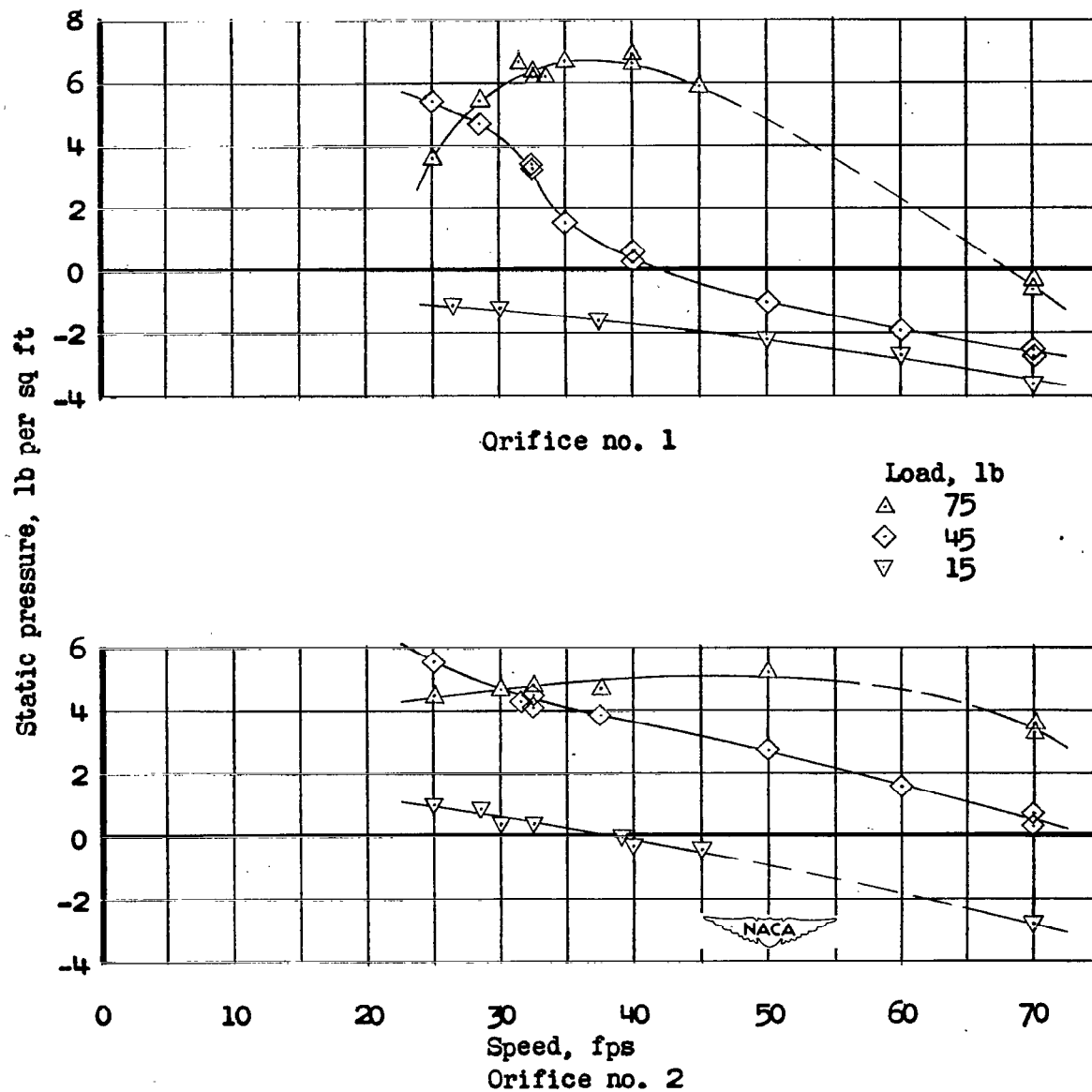
(b) Low-power condition.

Figure 5.- Concluded.



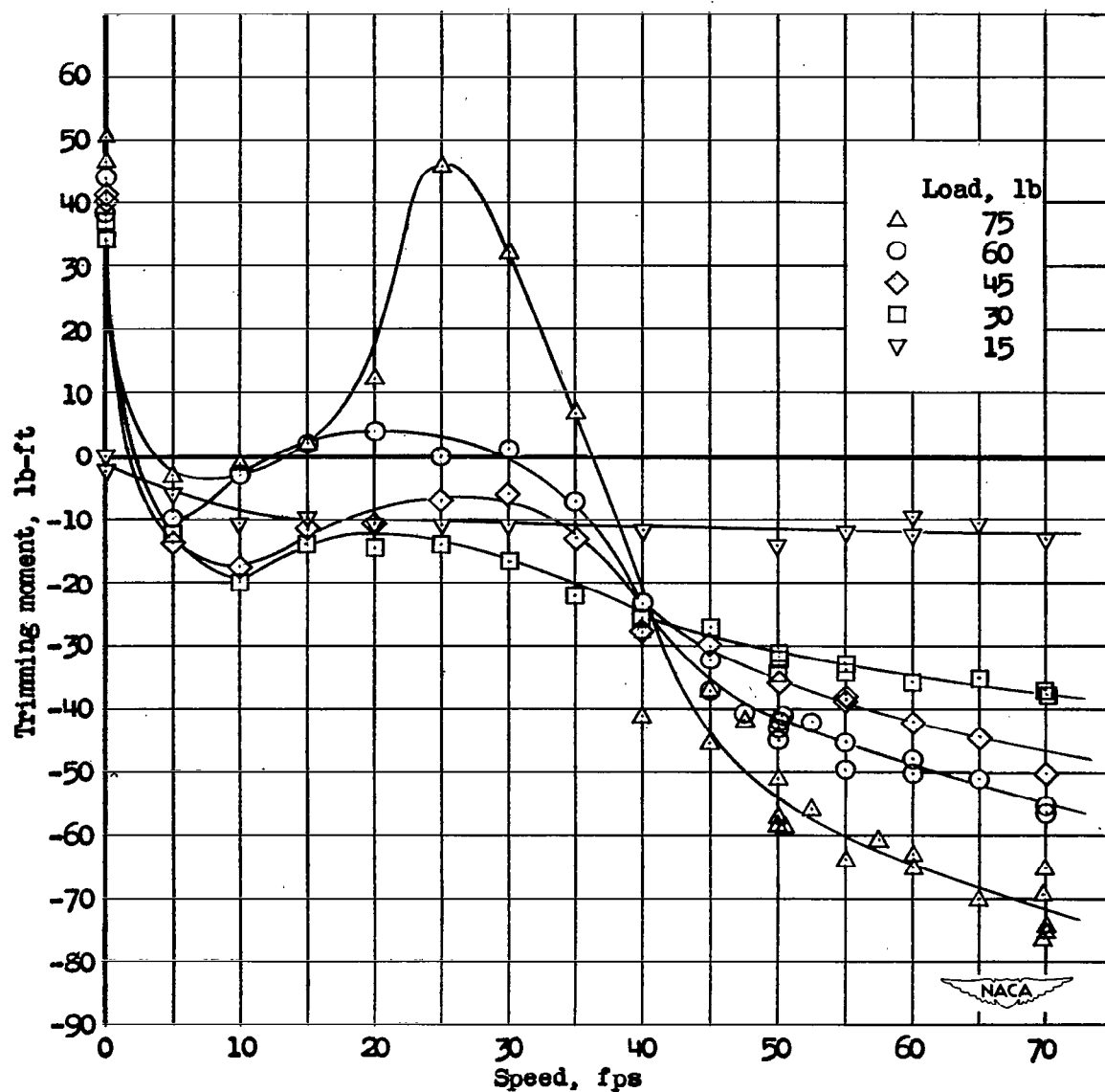
(a) High-power condition.

Figure 6.- Variation of tunnel pressures with speed. Model 171A-2.



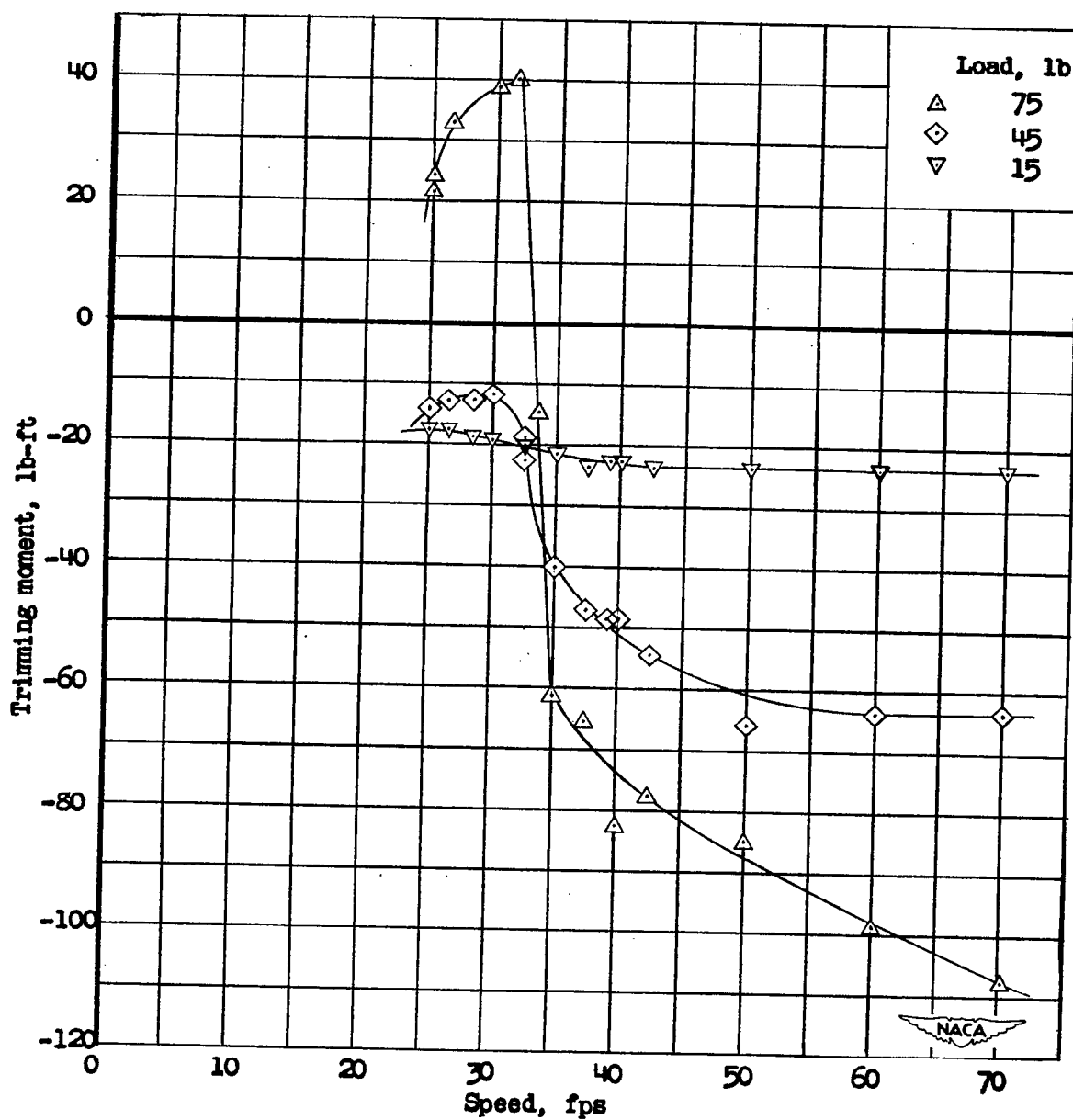
(b) Low-power condition.

Figure 6.- Concluded.



(a) High-power condition.

Figure 7.- Variation of trimming moment with speed. Model 171A-2.



(b) Low-power condition.

Figure 7.- Concluded.

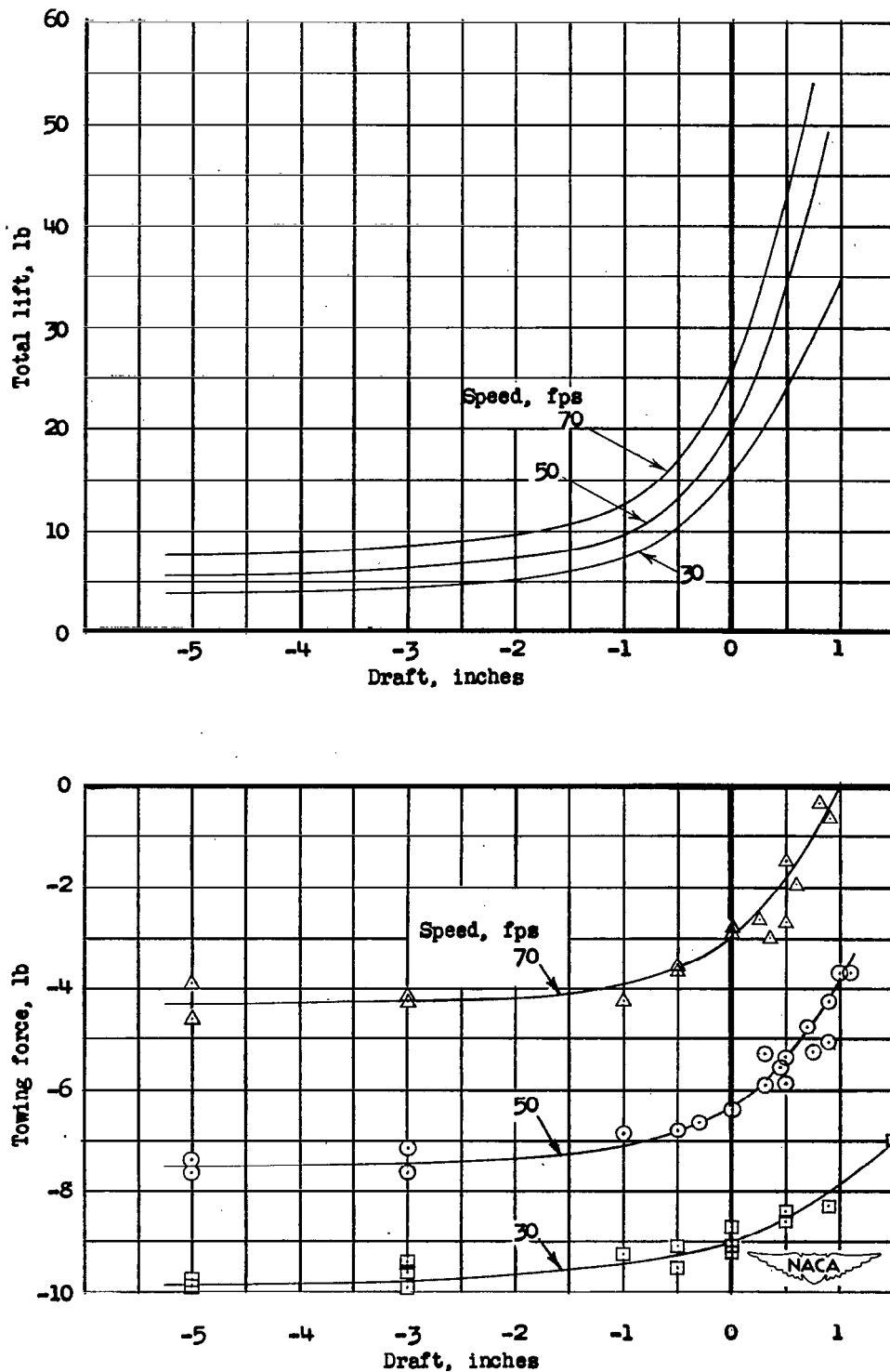


Figure 8.- Variation of towing force and towing lift with draft; high-power condition. Model 171A-2.



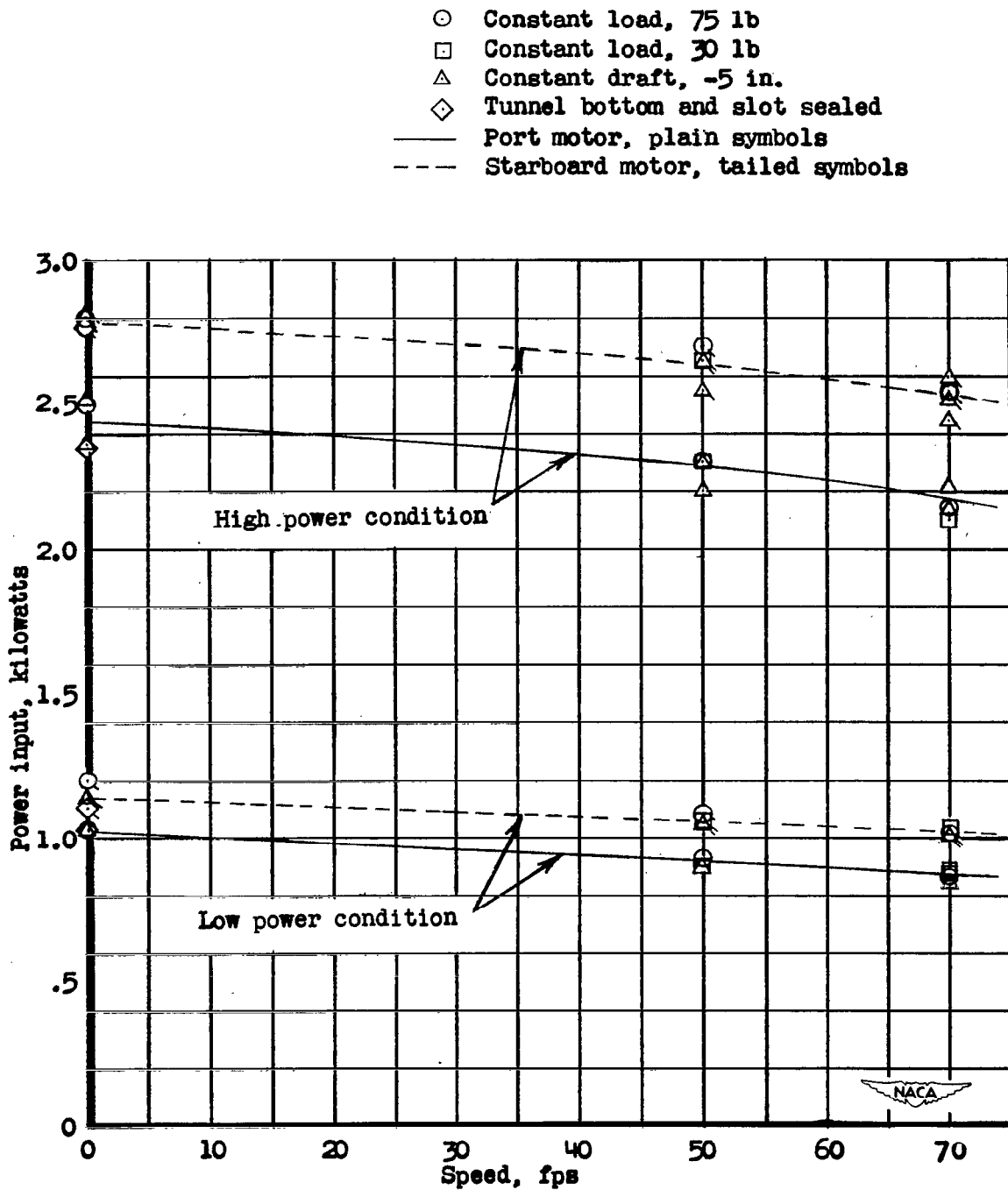


Figure 9.- Variation of power input to motors with speed. Model 171A-2.

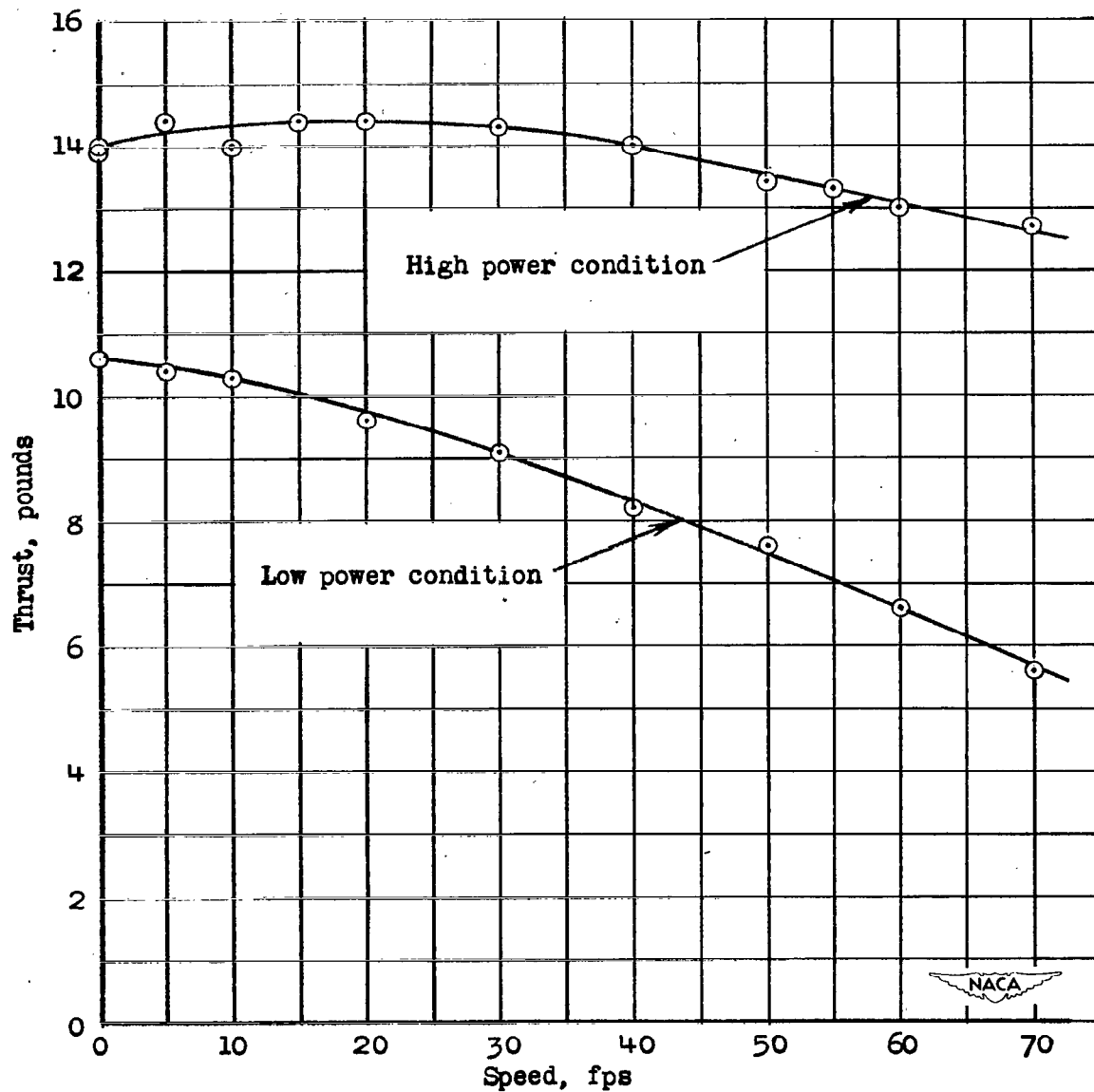
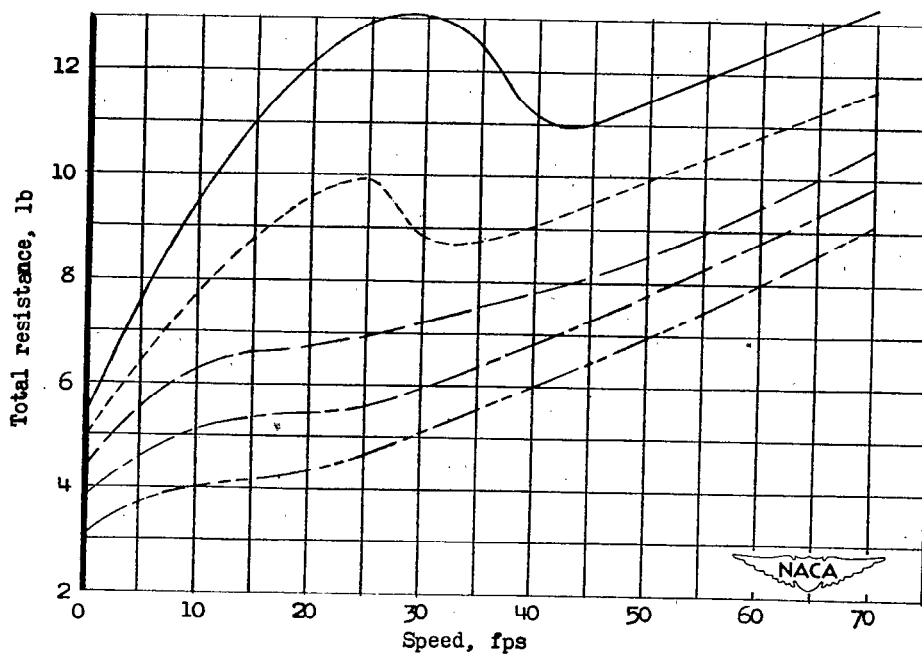
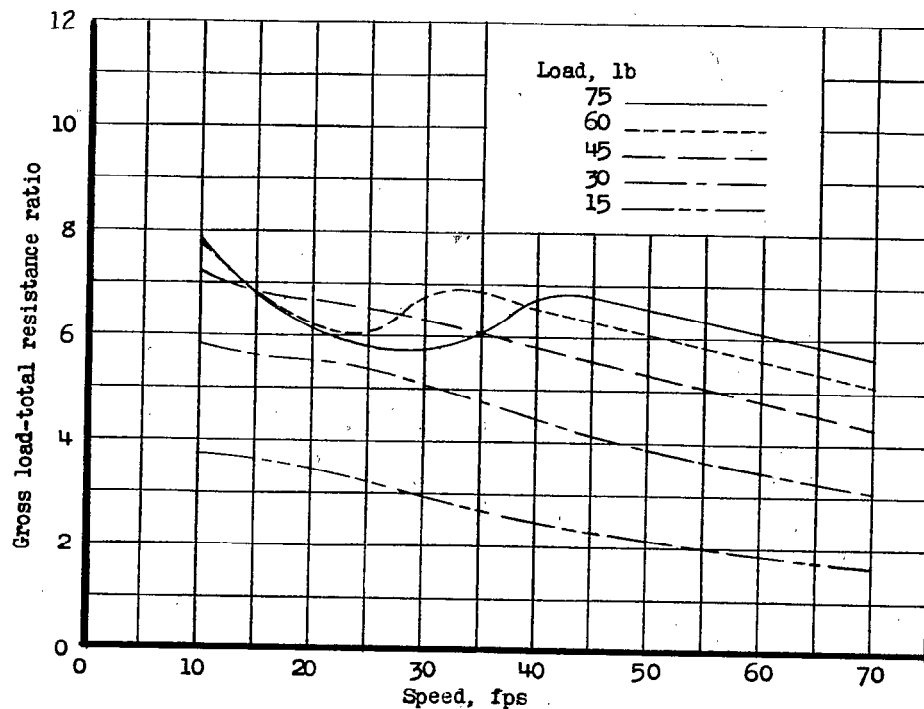
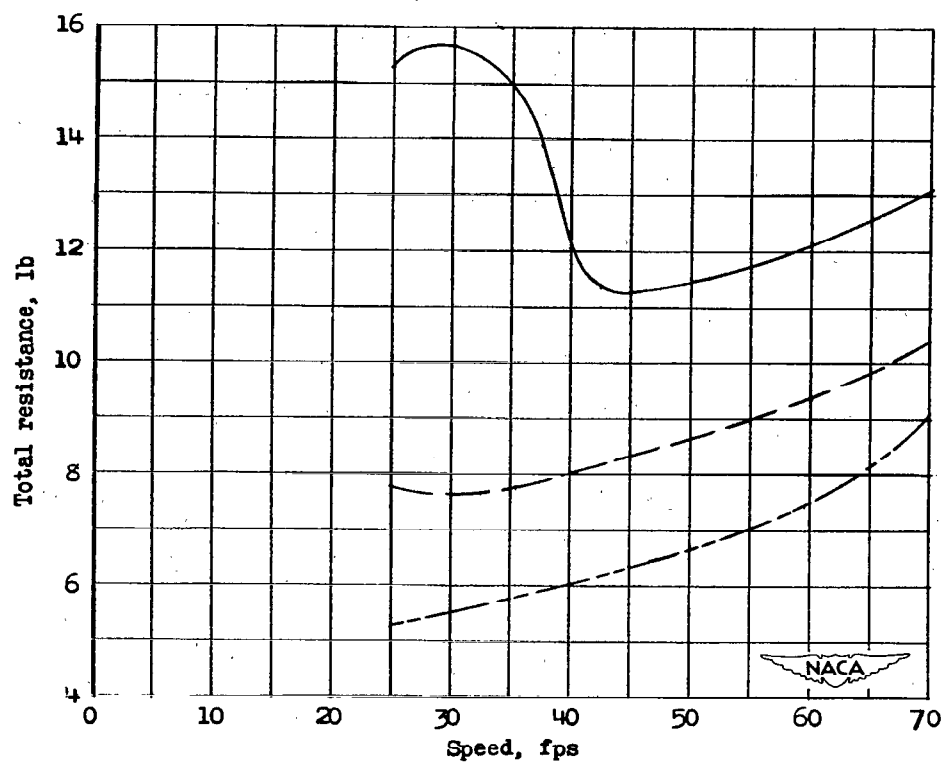
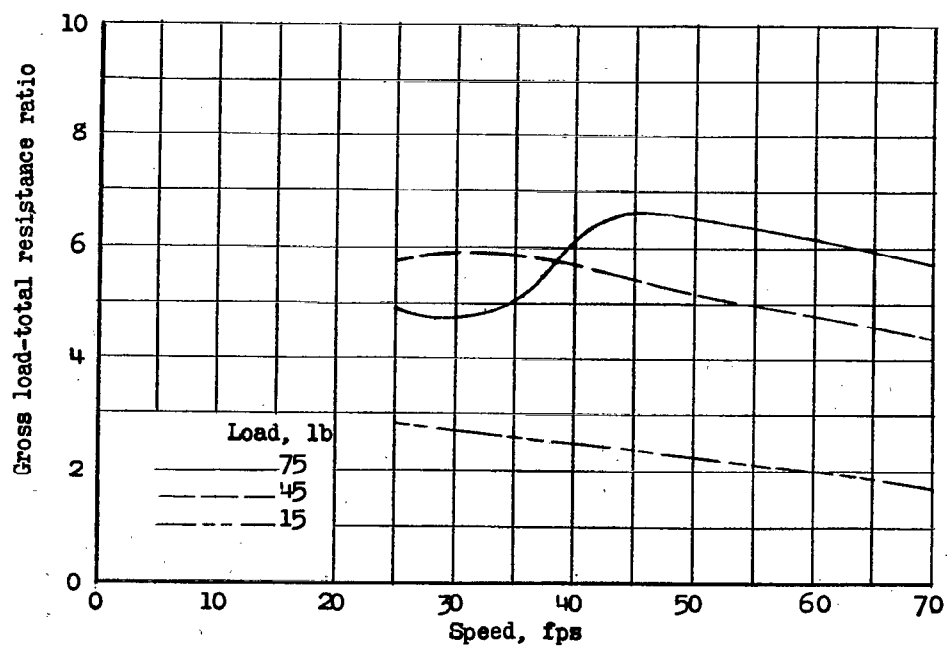


Figure 10.- Variation of thrust (propeller shaft tension) with speed.  
Model 171A-2.



(a) High-power condition.

Figure 11.- Variation of total resistance and gross load-total resistance ratio with speed. Model 171A-2.



(b) Low-power condition.

Figure 11.- Concluded.

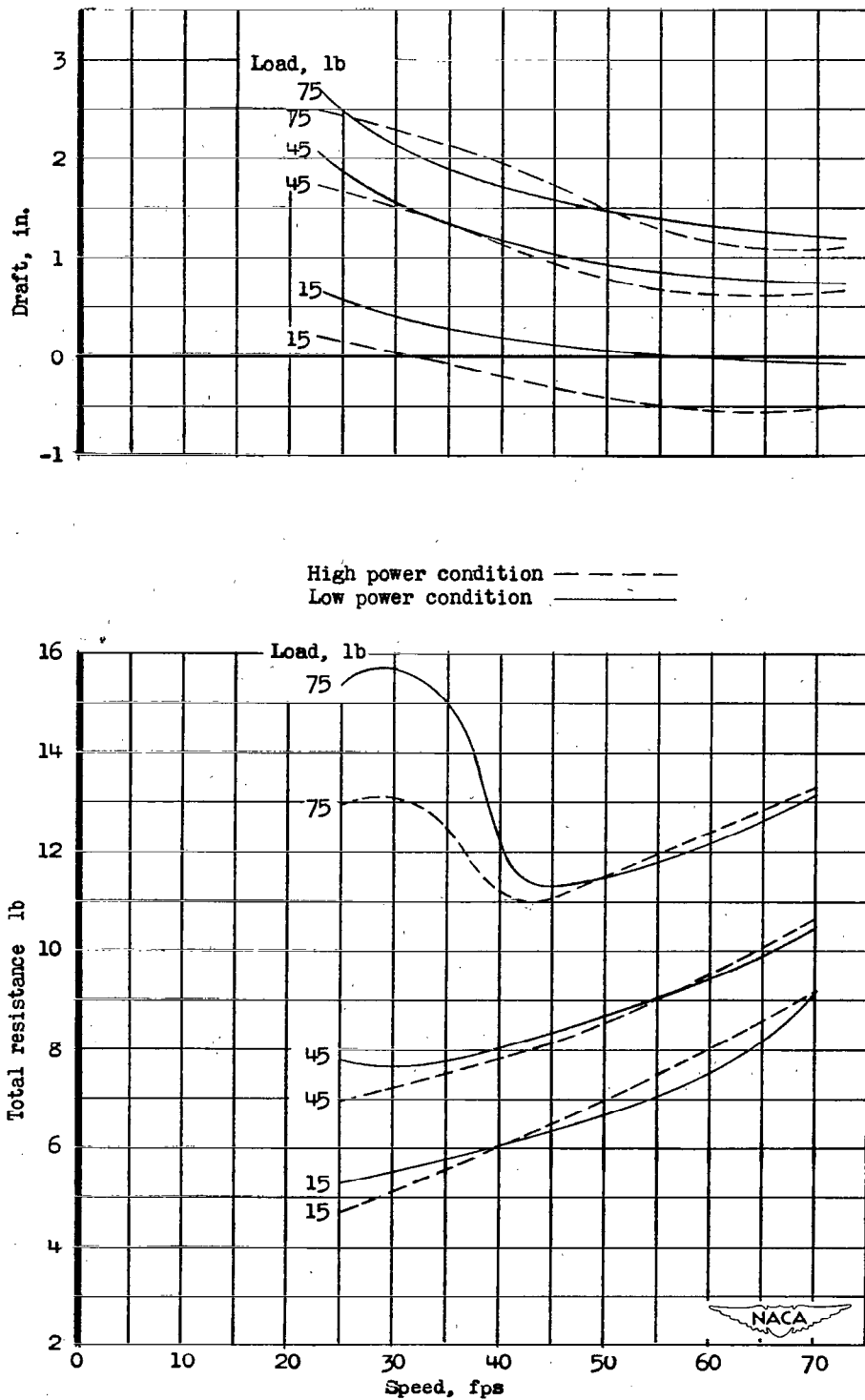


Figure 12.- Comparison of total resistance and draft for two values of static thrust. Model 171A-2.

NASA Technical Library



3 1176 01438 5331